Original Article

Regulation of Metabolic Responses by Adipocyte/Macrophage Fatty Acid–Binding Proteins in Leptin-Deficient Mice

Haiming Cao,[1] Kazuhisa Maeda,[1] Cem Z. Gorgun,[1] Hyo-Jeong Kim,[2] So-Young Park,[2] Gerald I. Shulman,[2,3] Jason K. Kim,[2] and Gökhan S. Hotamisligil[1]

Fatty acid–binding proteins (FABPs) are cytosolic fatty acid chaperones that play a critical role in systemic regulation of lipid and glucose metabolism. In animals lacking the adipocyte/macrophage FABP isoforms aP2 and mal1, there is strong protection against diet-induced obesity, insulin resistance, type 2 diabetes, fatty liver disease, and hypercholesterolemic atherosclerosis. On high-fat diet, FABP-deficient mice also exhibit enhanced muscle AMP-activated kinase (AMPK) and reduced liver stearoyl-CoA desaturase-1 (SCD-1) activities. Here, we performed a cross between aP2$^{-/-}$, mal1$^{-/-}$, and leptin-deficient (*ob/ob*) mice to elucidate the role of leptin action on the metabolic phenotype of aP2-mal1 deficiency. The extent of obesity in the *ob/ob*-aP2-mal1$^{-/-}$ mice was comparable with *ob/ob* mice. However, despite severe obesity, *ob/ob*-aP2-mal1$^{-/-}$ mice remained euglycemic and demonstrated improved peripheral insulin sensitivity. There was also a striking protection from liver fatty infiltration in the *ob/ob*-aP2-mal1$^{-/-}$ mice with strong suppression of SCD-1 activity. On the other hand, the enhanced muscle AMPK activity in aP2-mal1$^{-/-}$ mice was lost in the *ob/ob* background. These results indicated that both decreased body weight and enhanced muscle AMPK activity in aP2-mal1$^{-/-}$ mice are potentially leptin dependent but improved systemic insulin sensitivity and protection from liver fatty infiltration are largely unrelated to leptin action and that insulin-sensitizing effects of FABP deficiency are, at least in part, independent of its effects on total-body adiposity.
***Diabetes* 55:1915–1922, 2006**

From the [1]Department of Genetics and Complex Diseases, Division of Biological Sciences, Harvard School of Public Health, Boston, Massachusetts; the [2]Department of Internal Medicine, Endocrinology and Metabolism, Yale University School of Medicine, New Haven, Connecticut; and the [3]Howard Hughes Medical Institute, Yale University School of Medicine, New Haven, Connecticut.

Address correspondence and reprint requests to Gökhan S. Hotamisligil, MD, PhD, Harvard School of Public Health, 665 Huntington Ave., Boston, MA 02115. E-mail: ghotamis@hsph.harvard.edu.

Received for publication 15 November 2005 and accepted in revised form 5 April 2006.

H.C. and K.M. contributed equally to this work.

H.-J.K., S.-Y.P., and J.K.K. are currently affiliated with the Department of Cellular and Molecular Physiology, Pennsylvania State University College of Medicine, Hershey, Pennsylvania.

G.S.H. holds stock in Lipomics and Syndexa and has received an honorarium from Merck.

AMPK, AMP-activated kinase; FABP, fatty acid–binding protein; HGP, hepatic glucose production; SCD-1, stearoyl-CoA desaturase-1; SREBP, sterol regulatory element–binding protein.

DOI: 10.2337/db05-1496

Fatty acid–binding proteins (FABPs) constitute a family of cytosolic lipid chaperones sharing a conserved three-dimensional structure and exhibiting a distinct, tissue-specific expression pattern (1). FABP4 (aP2) is expressed predominantly in adipocytes and macrophages (2). Although aP2 exhibits higher affinity toward saturated long-chain fatty acids, it also binds to unsaturated fatty acids and retinoic acid (3,4). FABP5 (mal1) is detected more broadly, including in epidermal cells, brain, kidney, and lung, but is also expressed in adipocytes and macrophages, where it binds to fatty acids (5). Both aP2 and mal1 also interact with and stabilize leukotriene A4, which might play a role in their function in the macrophage (6). Recent studies through genetic manipulations in mice indicated that aP2 and mal1 play an important role in systemic metabolic homeostasis. For example, aP2-deficient mice are partially protected against obesity-induced insulin resistance in both dietary and genetic models (7,8). These animals are also resistant to atherosclerosis in hypercholesterolemic models (5,9). On the other hand, mal1-deficient mice exhibit a minor metabolic phenotype with improved systemic insulin sensitivity (10). Because, in the presence of aP2 deficiency, there is strong molecular compensation by mal1 in adipocytes (11), we have recently generated mice that express neither of these FABPs and observed a marked protection against diet-induced obesity, insulin resistance, type 2 diabetes, and fatty liver disease in these animals (12,13). The magnitude of this protection against metabolic disease was far more striking than the individual absence of either aP2 or mal1. In this model, we also identified increased muscle AMP-activated kinase (AMPK) activity and dramatically decreased liver stearoyl-CoA desaturase-1 (SCD-1) expression and activity as potential mechanisms that mediate the systemic effects of FABP deficiency (12,13). Interestingly, both AMPK and SCD-1 have been shown to be critical peripheral targets of leptin (14,15).

Mice homozygous for a spontaneous null mutation of leptin gene (*ob/ob*) exhibit hyperphagia and severe obesity. This *ob/ob* mice model also exhibits hyperglycemia, insulin resistance, hyperinsulinemia, glucose intolerance, and fatty infiltration of liver. Injection of leptin protein into *ob/ob* mice effectively reduces body weight and increases energy expenditure (16,17). Even though these effects of leptin were largely attributed to its action on central nervous system, two peripheral targets of leptin have been

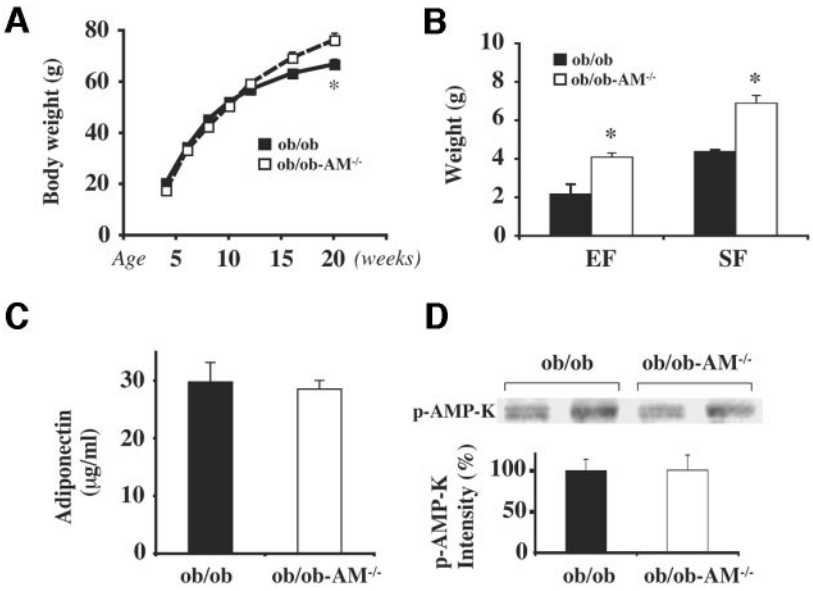

FIG. 1. Regulation of total body weight and adiposity in the *ob/ob*-aP2-mal$^{-/-}$ mice. *A*: Body weight curves of *ob/ob*-aP2-mal$^{-/-}$ (*ob/ob*-AM$^{-/-}$) mice and *ob/ob* controls (n = 10). *P < 0.01. *B*: Weight of epididymal (EF) and subcutaneous (SF) adipose tissues in *ob/ob*-aP2-mal1$^{-/-}$ mice and *ob/ob* controls (n = 5). *P < 0.05. *C*: Plasma adiponectin levels in *ob/ob*-aP2-mal1$^{-/-}$ mice and *ob/ob* controls at 16 weeks of age. *D*: Phosphorylation of AMPK in soleus muscle of *ob/ob* and *ob/ob*-AM$^{-/-}$ mice.

identified to play important roles in regulating energy homeostasis. Leptin robustly suppress SCD-1 expression in liver, and the increased SCD-1 expression and activity in the *ob/ob* mice has been proposed as an important mechanism underlying excess lipid accumulation in the liver (15). Leptin also activates AMPK activity and promotes fatty acid oxidation in skeletal muscle (14). Both SCD-1 and AMPK are significantly regulated in FABP deficiency, suggesting a link between these lipid-binding proteins and peripheral leptin action (12). Interestingly, however, circulating leptin level is significantly lower in FABP-deficient mice compared with wild-type controls on high-fat diet. This observation suggests either that FABP deficiency enhances leptin actions at peripheral target tissues, so that despite lower hormone concentrations similar or enhanced activity is generated, or that altered metabolic responses in FABP-deficient mice are independent of leptin function and involve other pathways and mechanisms.

In this study, we attempted to address these possibilities by studying the impact of lack of aP2 and mal1 on obesity and insulin sensitivity in a model of leptin deficiency. For this, we intercrossed aP2-, mal1-, and leptin-deficient *ob/ob* mice (18) and examined metabolic responses in the resulting animals. In this setting, despite developing severe obesity to a similar extent as the *ob/ob* controls, aP2-mal1–deficient mice were strikingly protected against systemic insulin resistance, type 2 diabetes, and hepatosteosis. In addition, the FABP deficiency–related increase in AMPK activity in muscle was no longer observed in the *ob/ob* background, but the robust suppression of liver SCD-1 activity was maintained. These results indicate that the impact of FABP deficiency on systemic insulin action and fatty liver disease is, at least in part, independent of total-body adiposity and leptin activity.

RESEARCH DESIGN AND METHODS

Generation of *ob/ob*-aP2$^{+/+}$mal1$^{+/+}$ and *ob/ob*-aP2$^{-/-}$mal1$^{-/-}$ mice. Mice deficient in aP2 and/or mal1 were generated as previously described (10,19). All mice were backcrossed >12 generations into the C57BL/6J genetic background. These aP2$^{-/-}$, mal1$^{-/-}$, or aP2$^{-/-}$mal1$^{-/-}$ mice were then intercrossed with heterozygote animals in the *ob* (leptin) locus (OB/ob-C57BL/6J) to generate double and triple heterozygotes (*OB/ob*-aP2$^{+/-}$, *OB/ob*-mal1$^{+/-}$, or *OB/ob*-aP2$^{+/-}$mal1$^{+/-}$). These mice were then intercrossed to generate *OB/ob*-aP2$^{-/-}$, *OB/ob*-mal1$^{-/-}$, *OB/ob*-aP2$^{-/-}$mal1$^{-/-}$, or aP2$^{+/+}$mal1$^{+/+}$ mice, which subsequently served as parents to lean and obese (*OB/OB* and *ob/ob*, respectively) animals either wild type (aP2$^{+/+}$mal1$^{+/+}$) or null (aP2$^{-/-}$, mal1$^{-/-}$ or aP2$^{-/-}$mal1$^{-/-}$) in the aP2 and mal1 locus.

Biochemical assays and insulin and glucose tolerance tests. Tolerance tests were performed on male mice after 6-h daytime food withdrawal. Insulin and glucose solutions were injected into peritoneal cavity at doses of 0.5 unit/kg and 1.0 ml/kg (1 mol/l solution), respectively. Blood was collected via tail vein at different time points, and glucose levels were measured by the use of a Glucometer (Precision). Plasma insulin and adiponectin levels were measured with radioimmunoassays for rat insulin and mouse adiponectin (Linco Research). Serum lipid concentrations were determined by established assays as previously described (10,20). Triglyceride in liver tissue was determined using a commercial kit (Determiner TG; Kyowa Medex, Tokyo, Japan).

Hyperinsulinemic-euglycemic clamp and cellular glucose uptake studies. Hyperinsulinemic-euglycemic clamp studies were performed essentially as described previously (21). Briefly, after overnight fast (~15 h), a 2-h hyperinsulinemic-euglycemic clamp was conducted with a continuous infusion of insulin (15 pmol · kg^{-1} · min^{-1}, Humulin; Eli Lilly, Indianapolis, IN) and variable infusion of 20% glucose (21). Basal and insulin-stimulated whole-body glucose turnover was estimated with a continuous infusion of [3-^{3}H]glucose (Perkin Elmer Life and Analytical Sciences, Boston, MA) for 2 h before and throughout the clamps (21). To estimate insulin-stimulated glucose uptake in individual tissues, 2-deoxy-D-[1-^{14}C]glucose (Perkin Elmer Life and Analytical Sciences) was administered as a bolus (10 μCi) at 75 min after the start of clamps. At the end of clamps, mice were anesthetized and tissues were taken for biochemical and molecular analysis (21).

For glucose uptake experiments in primary adipocytes, epididymal fat pads *ob/ob* or *ob/ob*-aP2-mal$^{-/-}$ mice (n = 5–6) were collected and digested with collagenase. The floating adipocytes were washed three times with Krebs-Ringer phosphate isolation buffer containing 20 mmol/l HEPES, pH 7.4, 2.5% BSA, 200 μmol/l adenosine, and 5 mmol/l glucose. A cell suspension (200 μl) was incubated with 2-deoxy-D-[1-^{14}C]glucose with or without 100 nmol/l insulin at 37°C for 30 min. After the incubation, the uptake was terminated by adding ice-cold stop solution containing 0.1% BSA and 200 μmol/l phloretin in the isolation buffer. The cell suspension was then transferred onto a Whatman glass filter, washed three times with ice-cold PBS, and counted using a liquid scintillation counter.

Immunoblotting. Lysates prepared from soleus muscle, adipose tissue, and liver samples were separated with SDS-PAGE gels. Phosphorylation of the α-subunit of AMPK was determined with a phospho-specific antibody recognizing both the α1 and α2 isoforms of the catalytic subunit of AMPK, which are phosphorylated on threonine 172 (Cell Signaling). Total protein levels of AMPK were determined using an antibody for both α1 and α2 subunits of AMPK (Cell Signaling). Phosphorylated AKT and total AKT were detected with antibodies for pAKT (Thr 473) and AKT, respectively (Cell Signaling). Full-length sterol regulatory element–binding protein 1 (SREBP1) was detected in whole-cell lysates prepared from liver tissues of *ob/ob* and *ob/ob*-aP2$^{-/-}$mal1$^{-/-}$ mice with an antibody against mouse SREBP1 (a generous gift of Dr. Jay Horton, UT Southwestern Medical School). Three individual mice of each genotype were compared, and a representative blot is shown. Nuclear

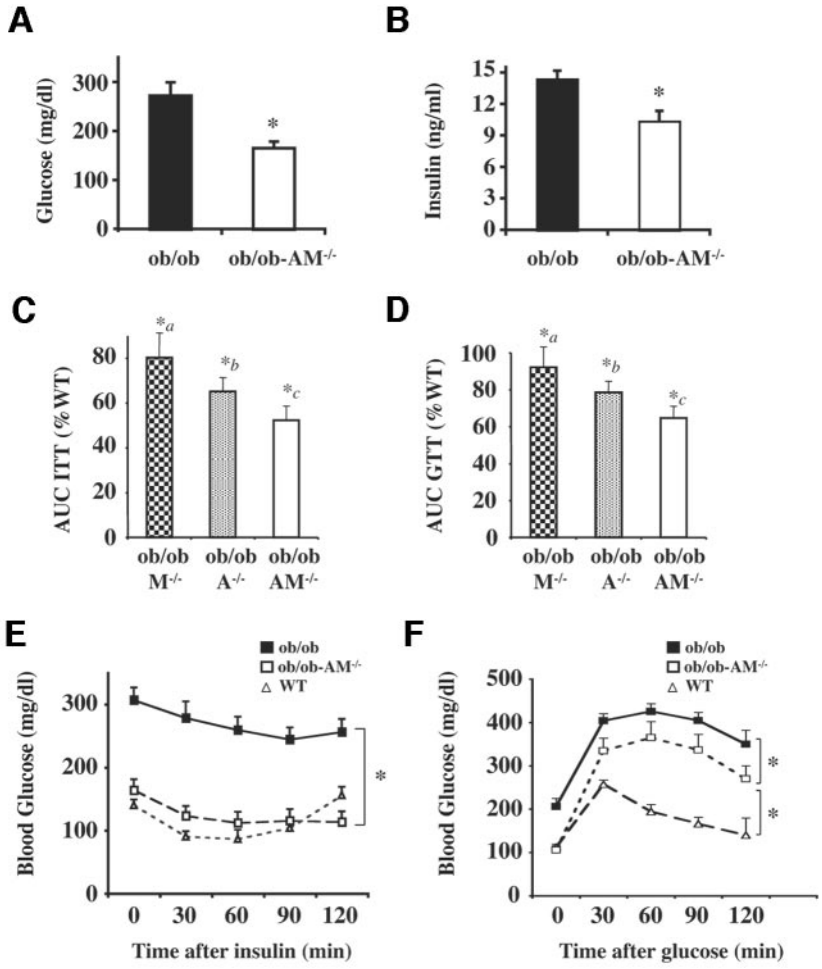

FIG. 2. Glucose metabolism in the *ob/ob*-aP2-mal$1^{-/-}$ mice. Plasma glucose (*A*) and insulin (*B*) levels in *ob/ob* and *ob/ob*-aP2-mal$1^{-/-}$ (*ob/ob*-AM$^{-/-}$) mice after 16-h fasting samples collected at 16 weeks of age. Insulin (*C*) and glucose (*D*) tolerance tests performed in *ob/ob*-mal$1^{-/-}$ (*ob/ob*-M$^{-/-}$, 13–14 weeks of age), *ob/ob*-aP2$^{-/-}$ (*ob/ob*-A$^{-/-}$, 14–15 weeks of age) and *ob/ob*-aP2-mal$1^{-/-}$ (*ob/ob*-AM$^{-/-}$, 17–18 weeks of age) and *ob/ob* (WT, 14–15 weeks) mice, n = 6–9 in each group. Data are presented as integrated area under the glucose disposal curves (AUC) for each genotype relative to *ob/ob* controls. *a = *ob/ob*-M$^{-/-}$ statistically significantly different from *ob/ob* (WT) and *ob/ob*-A$^{-/-}$; *b = *ob/ob*-A$^{-/-}$ is statistically significantly different from *ob/ob* (WT) and *ob/ob*-AM$^{-/-}$; *c = *ob/ob*-AM$^{-/-}$ is statistically significantly different from *ob/ob* (WT), *ob/ob*-A$^{-/-}$, and *ob/ob*-M$^{-/-}$ mice. Glucose disposal curves during insulin (*E*) and glucose (*F*) tolerance tests performed in *ob/ob*-aP2-mal$1^{-/-}$ and *ob/ob* animals. Tests performed similarly on lean wild-type mice were also included for comparison.

extracts were prepared from pooled liver tissues from three *ob/ob* or *ob/ob*-aP2$^{-/-}$mal$1^{-/-}$ mice (1.5 g each mouse) following procedures as described previously (22). Thirty micrograms of nuclear extracts were separated with SDS-PAGE gel and blotted with the same anti-SREBP1 antibody.

RNA extraction, Northern blotting, and real-time PCR analysis. Total RNAs were isolated from tissues using Trizol reagent (Invitrogen) and purified with RNAEasy kit (Qiagen). RNA (15 μg) was used for Northern blot analysis using a radioactively labeled SCD-1 probe. Ethidium bromide staining was used as control for loading and integrity of RNA samples. Reverse transcription was carried out with ThermoScript RT-PCR System (Invitrogen) using 1 μg RNA. Real-time PCR was performed on an iCycler iQ Detection System using iQ SYBR Green Supermix (Bio-Rad Laboratories). The PCR thermal cycling program was as follows: 2 min 30 s at 95°C for enzyme activation, 40 cycles of 15 s at 95°C, 30 s at 58°C, and 1 min at 72°C for extension. Melting curve analysis was performed to confirm the real-time PCR products. All quantitations were normalized to the 18S rRNA level. Primer sequences used are available upon request.

Statistical analysis. Two-tailed, two-sample, unequal-variance Student's t tests were used to assess statistical significance, and $P < 0.05$ was the accepted level of statistical significance.

RESULTS

Body weight and adiposity in *ob/ob*-aP2-mal$1^{-/-}$ mice. We intercrossed aP2-mal$1^{-/-}$ mice with the *ob/ob* model of genetic obesity resulting from leptin deficiency. These intercrosses produced progeny at the expected Mendelian ratios. The growth curves of these animals are shown in Fig. 1*A*. Unlike the profile seen on high-fat diet (12), the body weights of *ob/ob*-aP2-mal$1^{-/-}$ mice were indistinguishable from the *ob/ob* animals until 20 weeks of age by which time *ob/ob*-aP2-mal$1^{-/-}$ mice were even heavier than the *ob/ob* controls. At 20 weeks of age, there was also increased adiposity in *ob/ob*-aP2-mal$1^{-/-}$ mice evident at both epididymal and subcutaneous fat depots (Fig. 1*B*). Hence, the reduced body weight and adiposity phenotype observed in the aP2-mal$1^{-/-}$ mice in the dietary obesity model was completely lost on the *ob/ob* background. There was also no difference in the circulating levels of adiponectin between *ob/ob*-aP2-mal$1^{-/-}$ mice compared with *ob/ob* controls (Fig. 1*C*). In metabolic and indirect calorimetry studies, we also did not observe any difference in food intake, physical activity levels, or energy consumption between genotypes (data not shown).

We have previously demonstrated that aP2-mal1–deficient mice on high-fat diet have increased AMPK activity in skeletal muscle compared with wild-type animals, which might contribute to the reduced weight gain on high-fat diet (12). Because leptin has recently been shown to activate AMPK activity in muscle (14) and the weight difference was no longer evident in the aP2-mal$1^{-/-}$ mice in the leptin-deficient background, we examined phosphorylation of AMPK in muscle tissue in the *ob/ob* background. Interestingly, and unlike what has been seen in the dietary obesity model (12), we found no difference in muscle tissue AMPK phosphorylation between *ob/ob* and *ob/ob*-aP2-mal$1^{-/-}$ mice (Fig. 1*D*). These findings are consistent with the model that FABP-mediated regulation of both AMPK activity and body weight does not occur in the absence of leptin activity.

Glucose metabolism in *ob/ob* and *ob/ob*-aP2-mal$1^{-/-}$ mice. An important question is to address whether the changes in insulin sensitivity seen in aP2-mal1 deficiency are secondary to changes in body weight. If this is the

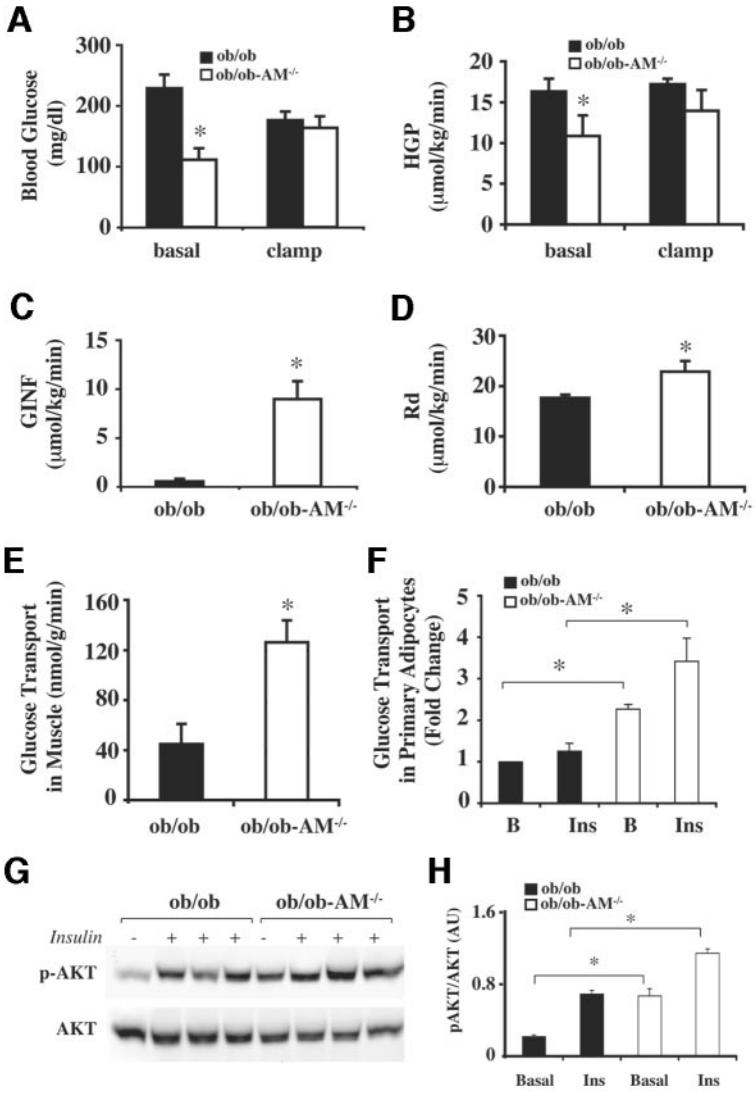

FIG. 3. Whole-body glucose metabolism in the *ob/ob*-aP2-mal$^{-/-}$ mice. *A*: Overnight fasted (~15 h) plasma glucose (basal) and during hyperinsulinemic-euglycemic clamp. *B*: Basal and clamped HGP. *C*: Steady-state glucose infusion rate (GINF) obtained from averaged rates of 90–120 min of clamps. *D*: Insulin-stimulated whole-body glucose turnover (Rd). *E*: Insulin-stimulated glucose uptake in skeletal muscle (gastrocnemius) during clamps. *F*: Basal (B) or insulin-stimulated (Ins) glucose uptake in isolated primary adipocyte. Results are fold changes compared with basal glucose uptake in adipocytes of *ob/ob* mice. *$P < 0.05$. Basal and insulin-stimulated AKT phosphorylation in adipose tissue (*G*) and quantitation of the basal and insulin-stimulated AKT phosphorylation in adipose tissues (*H*). AU, arbitrary unit.

case, protection against insulin resistance should not be observed in the *ob/ob* background. The *ob/ob*-aP2-mal1$^{-/-}$ mice provide a suitable model for addressing this question because they have increased body weight compared with *ob/ob* mice. Hence, we examined insulin sensitivity in *ob/ob*-aP2-mal1$^{-/-}$ and *ob/ob*-aP2-mal1$^{+/+}$ mice. As expected, *ob/ob* mice developed mild hyperglycemia with severe hyperinsulinemia at 20 weeks of age. In contrast, *ob/ob*-aP2-mal1$^{-/-}$ mice remained euglycemic and had significantly lower blood insulin concentrations compared with *ob/ob* controls (Fig. 2*A* and *B*). We next performed insulin and glucose tolerance tests in these animals and also included *ob/ob*-aP2$^{-/-}$ and *ob/ob*-mal1$^{-/-}$ mice to compare responses in individual deficiency of each FABP with combined aP2-mal1 deficiency in the *ob/ob* background. The hypoglycemic response to insulin was lower in all of the FABP-deficient *ob/ob* models compared with *ob/ob* mice (shown as quantitation of the responses by integrating the area under the disposal curves; Fig. 2*C*). This increase in insulin sensitivity in insulin tolerance test was most dramatic in *ob/ob* aP2-mal1$^{-/-}$ mice, and glucose disposal curves of this group were indistinguishable from those of lean animals (Fig. 2*E*). Insulin sensitivity was also increased in the *ob/ob*-aP2$^{-/-}$ and *ob/ob*-mal1$^{-/-}$ mice compared with *ob/ob* controls. The magnitude of increase in insulin responsiveness relative to the *ob/ob* controls in the *ob/ob*-aP2$^{-/-}$ mice (35%) was smaller than the *ob/ob*-aP2-mal1$^{-/-}$ mice (48%) but greater than the *ob/ob*-mal1$^{-/-}$ (20%) animals (Fig. 2*C*). Glucose tolerance test also revealed a similar pattern but exhibited a partial effect of FABP deficiency (Fig. 2*D* and *F*). The increase in glucose disposal rates in the *ob/ob*-aP2$^{-/-}$ mice (20%) was smaller than the *ob/ob*-aP2-mal1$^{-/-}$ mice (35%) but greater than the *ob/ob*-mal1$^{-/-}$ (7%) animals (Fig. 2*D*). These results demonstrate that aP2-mal1 deficiency resulted in strong but incomplete protection from insulin resistance in the *ob/ob* background and, similar to the dietary model, the magnitude of this effect is greater than each of the single deficiency of aP2 or mal1 in the *ob/ob* model.

To determine organ-specific changes in glucose metabolism in vivo in the *ob/ob*-aP2-mal1$^{-/-}$ mice and to compare the impact of FABP deficiency with diet-induced insulin resistance, we performed hyperinsulinemic-euglycemic clamp studies. The basal glucose level observed in this study was again significantly lower in *ob/ob*-aP2-mal1$^{-/-}$ mice than that of *ob/ob* controls (Fig. 3*A*). The basal hepatic glucose production (HGP) in *ob/ob*-aP2-mal1$^{-/-}$ mice showed a 33% reduction compared with controls, and this could be one of the reasons that *ob/ob*-aP2-mal1$^{-/-}$ mice maintain euglycemia (Fig. 3*B*). In

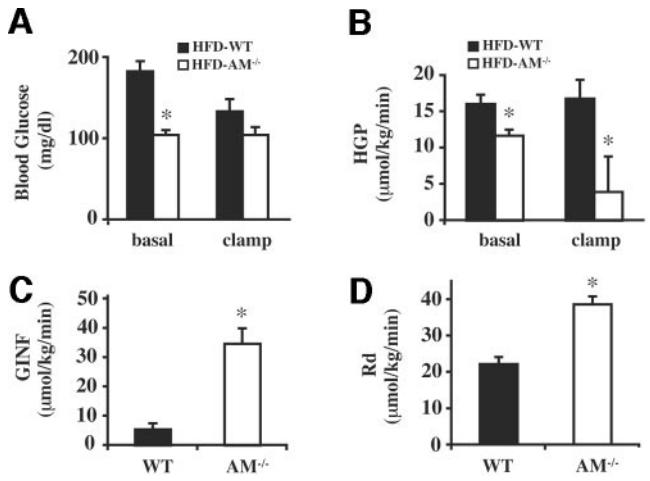

FIG. 4. Whole-body glucose metabolism in the aP2-mal$^{-/-}$ mice fed high-fat diet. *A*: Plasma glucose during basal and hyperinsulinemic-euglycemic clamp periods. *B*: Basal and clamp HGP. *C*: Steady-state glucose infusion rate (GINF). *D*: Insulin-stimulated whole-body glucose turnover (Rd). *$P < 0.05$.

contrast, insulin-stimulated HGP during clamps did not show significant difference between *ob/ob* and *ob/ob*-aP2-mal1$^{-/-}$ mice. These data suggest that the impact of FABP deficiency on HGP in the *ob/ob* mice might be predominately at the basal level. The steady-state glucose infusion rate during clamps was markedly elevated in *ob/ob*-aP2-mal1$^{-/-}$ mice compared with the *ob/ob* controls (Fig. 3*C*) despite sustained hepatic insulin resistance, suggesting that *ob/ob*-aP2-mal1$^{-/-}$ mice have enhanced glucose metabolism in other organs. Consistent with this, insulin-stimulated whole-body glucose turnover was significantly increased in *ob/ob*-aP2-mal1$^{-/-}$ mice compared with *ob/ob* mice (Fig. 3*D*). Increased whole-body insulin sensitivity was mostly due to a 2.5-fold increase in skeletal muscle glucose uptake in *ob/ob*-aP2-mal1$^{-/-}$ mice compared with *ob/ob* mice (Fig. 3*E*). Insulin-stimulated glycolysis and glycogen synthesis in skeletal muscle were also increased in *ob/ob*-aP2-mal1$^{-/-}$ mice. The rate of muscle glycolysis was 107 ± 18 nmol $\cdot$ g^{-1} $\cdot$ min^{-1} in *ob/ob*-aP2-mal1$^{-/-}$ mice compared with 40 ± 16 nmol $\cdot$ g^{-1} $\cdot$ min^{-1} in *ob/ob* controls ($P < 0.01$). Similarly, glycogen synthesis rate in *ob/ob*-aP2-mal1$^{-/-}$ mice (20 ± 5 nmol $\cdot$ g^{-1} $\cdot$ min^{-1}) also shows a threefold increase compared with that in *ob/ob* mice (6 ± 2 nmol $\cdot$ g^{-1} $\cdot$ min^{-1}).

In an independent experiment, we also determined glucose uptake by isolated primary adipocytes from *ob/ob* or *ob/ob*-aP2-mal1$^{-/-}$ mice and again found *ob/ob*-aP2-mal1$^{-/-}$ mice have significantly increased basal and insulin-stimulated glucose uptake in adipocytes (Fig. 3*F*). Taken together, our data indicate that *ob/ob*-aP2-mal1$^{-/-}$ mice have improved glucose homeostasis with decreased HGP and significantly enhanced insulin sensitivity and glucose metabolism in skeletal muscle and adipose tissues. To directly assess insulin signaling in *ob/ob*-aP2-mal1$^{-/-}$ mice, we also determined basal and insulin-stimulated AKT phosphorylation in the adipose tissues of *ob/ob*-aP2-mal1$^{-/-}$ mice. Consistent with increased glucose uptake, insulin-stimulated AKT phosphorylation was significantly increased both at baseline and insulin-stimulated state in the adipose tissues of *ob/ob*-aP2-mal1$^{-/-}$ mice compared with *ob/ob* controls (Fig. 3*G* and *H*).

As a comparison, we also performed insulin clamp studies on wild-type and aP2-mal$^{-/-}$ mice after short-term (3 weeks) high-fat feeding. aP2-mal$^{-/-}$ mice fed with high-fat diet exhibited markedly decreased basal glucose level, as we demonstrated before (Fig. 4*A*) (12), that may be partly due to reduced basal HGP in fat-fed aP2-mal$^{-/-}$ mice compared with fat-fed wild-type mice (Fig. 4*B*). High-fat feeding caused hepatic insulin resistance in the wild-type mice, as indicated by significantly diminished insulin-mediated suppression of basal HGP (Fig. 4*B*). In contrast, diet-induced hepatic insulin resistance was partially rescued in aP2-mal$^{-/-}$ mice, as reflected by significantly reduced clamp HGP compared with the fat-fed wild-type mice (Fig. 4*B*). The glucose infusion rate during clamp was fivefold higher in aP2-mal1$^{-/-}$ mice than that in controls (Fig. 4*C*), and this was due to the combined effects of decreased HGP and increased whole-body glucose uptake in aP2-mal1$^{-/-}$ mice (Fig. 4*D*). Consistent with the findings in the *ob/ob* mice, increased insulin sensitivity in fat-fed aP2-mal1$^{-/-}$ mice was due to twofold increase in insulin-stimulated glucose uptake in skeletal muscle compared with fat-fed wild-type mice (data not shown). When compared side by side, it appears that the improvement of insulin sensitivity in aP2-mal1–deficient mice is greater in diet-induced obesity than that in genetic obesity. These results suggest that the insulin-sensitizing effect of FABP deficiency is partially offset by the excess adiposity in leptin-deficient mice.

Fatty liver disease in the *ob/ob* and *ob/ob*-aP2-mal1$^{-/-}$ mice. Earlier studies demonstrated that aP2-mal1$^{-/-}$ mice were essentially completely protected against diet-induced fatty infiltration of liver (12). Despite their enlarged fat depots, we observed a 33.4% reduction in liver size in *ob/ob*-aP2-mal1$^{-/-}$ mice compared with *ob/ob* controls (Fig. 5*A*). Consistent with the reduction in liver weight, histological examination of liver sections revealed a dramatic reduction in fatty infiltration in *ob/ob*-aP2-mal1$^{-/-}$ mice compared with the *ob/ob* animals (Fig. 5*D*). Quantification of liver triglyceride content also revealed a significant (27%) decrease in *ob/ob*-aP2-mal1$^{-/-}$ mice compared with *ob/ob* animals (Fig. 5*B*). The reduced triglyceride content in the livers of FABP-deficient *ob/ob* mice was not related to reduced lipid supply to liver because portal vein fatty acid concentrations in these animals were higher than *ob/ob* controls (Fig. 5*C*). This striking protection against fatty liver disease in the *ob/ob* background was comparable with that observed in FABP-deficient mice on high-fat diet (12).

To approach the underlying mechanisms for the protection against fatty liver diseases in aP2-mal1$^{-/-}$ mice, we examined the expression patterns of several key lipogenic genes. These experiments revealed a systemic decrease in the expression of a wide spectrum of genes involved in liver lipogenesis in the *ob/ob*-aP2-mal1$^{-/-}$ mice (Fig. 4*F*). These included acetyl-CoA carboxylase 1, fatty acid synthase, SCD-1, fatty acid elongase, mitochondria glycerol-phosphate acyltransferase, SPOT14, hydroxymethylglutaryl-CoA reductase, and hydroxymethylglutaryl-CoA synthase. Among these, SCD-1 is a key rate-limiting enzyme in triglyceride synthesis (23) and is subject to robust regulation by leptin in liver (15). We have also observed a marked (96%) suppression of the expression of this gene in the FABP-deficient animals on high-fat diet (12). Interestingly, SCD-1 expression was also markedly suppressed (75%) in the liver of *ob/ob*-aP2-mal1$^{-/-}$ mice compared with *ob/ob* controls (Fig. 5*E* and *F*), indicating that leptin activity cannot account for this FABP-mediated regulation. Interestingly, expression of SREBP family transcrip-

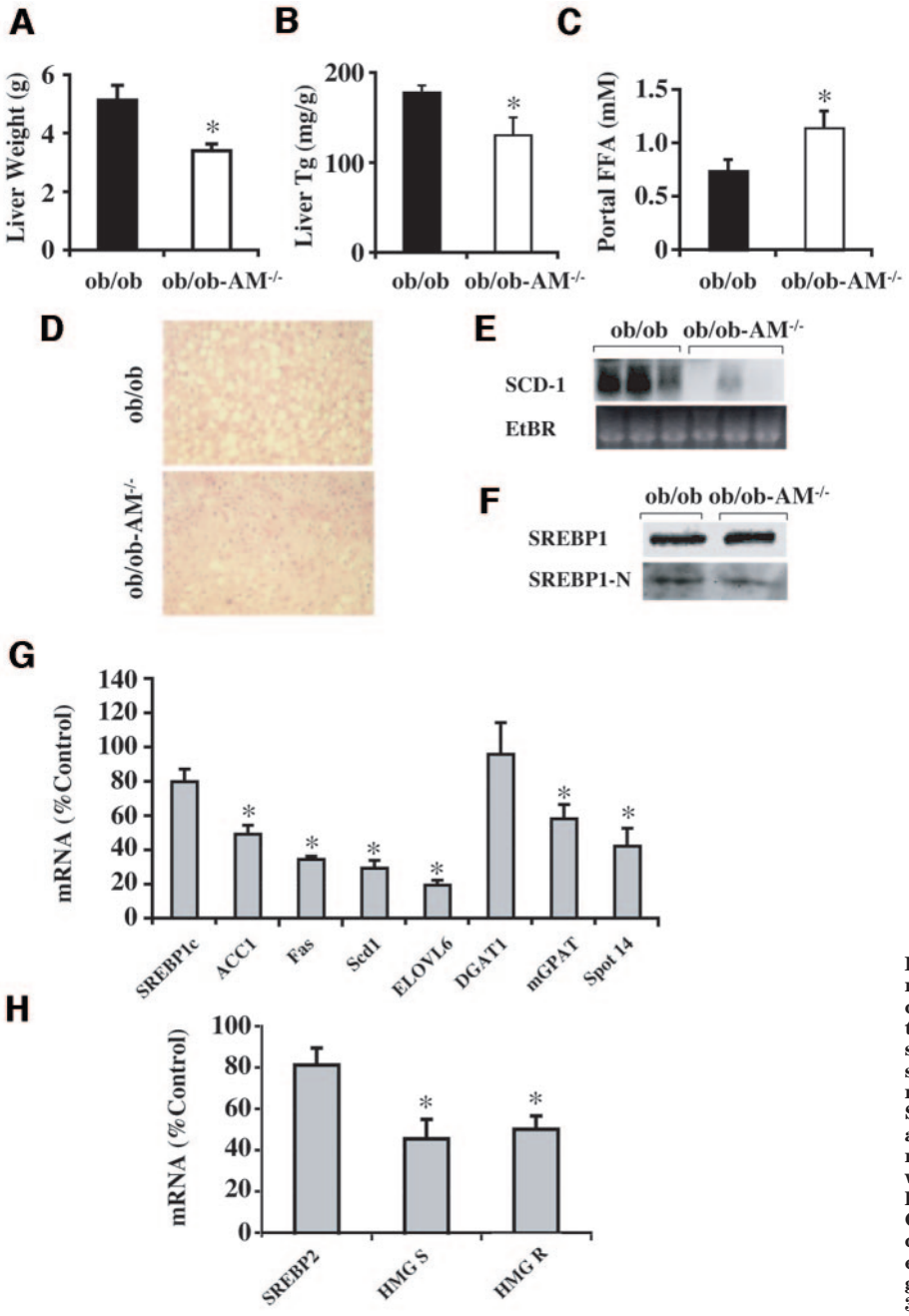

FIG. 5. Liver lipid metabolism in the *ob/ob*-aP2-mal$^{-/-}$ mice. Total wet weight (*A*) and triglyceride content (*B*) of liver tissue. *C*: Portal concentration of free fatty acids. *D*: Hematoxylin-eosin staining of liver sections (×250). *E*: SCD1 expression in the liver tissue of *ob/ob* and *ob/ob*-AM$^{-/-}$ mice. *F*: Full-length (SREBP1) and nuclear SREBP1 (SREBP1-N) in the liver tissue of *ob/ob* and *ob/ob*-AM$^{-/-}$ mice. *G* and *H*: Relative liver mRNA expression in *ob/ob*-AM$^{-/-}$ mice compared with *ob/ob* controls. ACC, acetyl-CoA carboxylase; FAS, fatty acid synthase; SCD-1, stearoyl-CoA desaturase; ELOVL6, elongation of very-long-chain fatty acid-6; DGAT1, acyl-CoA:diacylglycerol acyltransferase 1; mGPAT, mitochondria glycerol-phosphate acyltransferase; HMGCoA, 3-hydroxy-3-methylglutaryl CoA. *$P < 0.05$.

tion factors, SREBP1 and SREBP2, both slightly decreased, but this difference did not reach statistic significance (Fig. 5*F* and *G*). To determine the possibility that changes in SREBP processing might be responsible for the altered lipogenic gene expression, we also compared full-length and processed SREBP protein levels in the liver of *ob/ob* and *ob/ob*-aP2-mal1$^{-/-}$ mice (Fig. 5*H*). Full-length SREBP protein was unchanged in *ob/ob*-aP2-mal1$^{-/-}$ mice compared with *ob/ob* controls, and there was only a minor reduction in the processed form in liver tissues. These results suggest that changes in SREBP activity might not be the major mechanisms by which liver lipogenic gene expression is regulated by FABP deficiency.

DISCUSSION

In this study, we demonstrated that mice lacking the FABPs aP2 and mal1 develop severe obesity on the *ob/ob* genetic background but exhibit reduced insulin resistance and maintain euglycemia. These *ob/ob*-aP2-mal1$^{-/-}$ mice are also strikingly protected against fatty liver disease. Although the extent of the protection against insulin sensitivity in FABP-deficient animals appears to be smaller than that observed upon the high-fat feeding, the reversal of fatty liver disease is similar between the diet-induced and *ob/ob* models. In hyperinsulinemic-euglycemic clamp studies, the improved glucose homeostasis in the *ob/ob*-aP2-mal1$^{-/-}$ mice appears to be the combined result of increases in hepatic insulin action and insulin-stimulated glucose metabolism in peripheral tissues. Although significant, the magnitude of the increase in insulin sensitivity in FABP-deficient mice is smaller in the *ob/ob* background when compared with that observed in the high-fat diet–induced insulin resistance. In this high-fat diet feeding experiment, FABP deficiency can provide essentially com-

plete protection against systemic insulin resistance. In the *ob/ob* model, we did not detect a statistically significant difference in HGP under the clamp. Although this might be a difference in the extent of insulin sensitivity in the dietary and *ob/ob* models, it is also possible that the higher animal-to-animal fluctuations in the leptin-deficient background might have prevented the detection of the difference at a statistically significant level. In fact, the phosphorylation of AKT is increased in the livers of *ob/ob*-aP2-mal1$^{-/-}$ animals compared with *ob/ob* controls, supporting this possibility (data not shown). Hence, the difference in the insulin sensitivity between models could be related to the severity of disease in the *ob/ob* mice or the involvement of leptin activity in this phenotype. Interestingly, the fatty liver phenotype and the associated changes in liver lipogenic gene expression are also similar between the FABP-deficient animals in the *ob/ob* background or on high-fat diet. These results indicate that leptin activity might be involved in some but not all phenotypes associated with FABP deficiency.

Increased muscle AMPK and decreased liver SCD-1 activity seen in FABP-deficient mice on high-fat diet have raised the possibility that FABP deficiency may modulate leptin actions. Neither in this study nor in our earlier work in dietary obesity were we able to demonstrate any changes in food intake in aP2-mal1$^{-/-}$ mice. Hence, the role of FABPs in this respect is likely to involve peripheral tissues and targets. In the leptin-deficient *ob/ob* model, FABP deficiency no longer yields enhanced AMPK activity in muscle, suggesting that this activity might relate to intact leptin action. We have previously shown that enhanced activation of AMPK in skeletal muscle is likely to be critical for body weight regulation in dietary obesity (12). Our findings here support this proposal by the simultaneous loss of both FABP-related body weight reduction and enhanced AMPK activity in *ob/ob* background. Adiponectin also stimulates fatty acid oxidation through AMPK activity (24), and transgenic expression or administration of recombinant adiponectin to animals might cause weight loss (25,26). In our previous studies using the high-fat diet model, we have observed a paradoxical decrease in adiponectin expression and serum levels in aP2-mal1–deficient animals (12). Interestingly, this decreased adiponectin production was not preserved in the *ob/ob* mice (Fig. 1*C*).

Unlike body weight regulation, protection against fatty liver disease and diabetes was preserved in the *ob/ob*-aP2-mal1$^{-/-}$ mice, indicating that these phenotypes are independent of leptin action. Increased release of free fatty acids from adipose tissue and their negative metabolic impact on muscle tissue have long been postulated as an important component of the link between obesity and insulin resistance (27,28). This aspect also appears to be similarly regulated between the dietary and *ob/ob* models with FABP deficiency because the aP2-mal1$^{-/-}$ mice have slightly higher circulating free fatty acids compared with wild-type controls but nevertheless maintain their insulin sensitivity and euglycemia (Table 1). These observations support the emerging concept that altered fatty acid profile or the downstream response pathways are the critical determinants of insulin sensitivity or other metabolic outcomes rather than the absolute amount of circulating lipids. Detailed analysis of lipid composition and metabolism of the *ob/ob*-aP2-mal1$^{-/-}$ mice is ongoing, and such studies should shed light on the impact of FABP-regulated alterations in fatty acid profile on insulin action

TABLE 1
Plasma lipid levels in *ob/ob* and *ob/ob*-AM$^{-/-}$ mice

	ob/ob	*ob/ob*-AM$^{-/-}$
Triglyceride (mg/dl)	151.59 ± 12.68	121.34 ± 4.61*
Total cholesterol (mg/dl)	259.18 ± 16.23	219.16 ± 6.54*
Glycerol (mmol/l)	0.77 ± 0.04	0.73 ± 0.05
Free fatty acid (mmol/l)	0.97 ± 0.09	1.31 ± 0.08*

Data are means ± SE. Biochemical measurements were performed at 16 weeks of age.

in the *ob/ob* genetic background. Interestingly, in a preliminary microarray analysis, we did not observe significant differences in the expression of the majority of the inflammatory gene products in adipose tissues of aP2-mal1$^{-/-}$ animals (data not shown). Although we have not made the comparable analysis in the dietary obesity models, it is possible that this aspect might also play into the differences between the magnitude of phenotypes or result from the lack of any weight reduction due to FABP deficiency in the *ob/ob* background. It is also possible that the phenotypic changes seen in this model are independent of adipose tissue inflammation. Further experiments will be needed to distinguish these possibilities.

The protection from fatty infiltration of liver may also offer novel insights into how adipose tissue effect liver lipid accumulation during the course of obesity. In the liver of aP2-mal1–deficient animals on high-fat diet, SCD-1 gene exhibits the most striking regulation with 96% reduction in the expression level compared with wild-type controls. SCD-1 is a major peripheral target of leptin, and SCD-1 suppression can generate effects on body weight and systemic metabolism (15). Most interestingly, liver SCD-1 expression in aP2-mal1–deficient mice on the *ob/ob* background was still markedly suppressed, demonstrating that FABP deficiency leads to marked downregulation of liver SCD-1 expression through a leptin-independent mechanism. Adiponectin also has no effects on liver SCD-1 level or activity, and no regulation of this gene is evident in adiponectin-deficient animals (data not shown). This raises the exciting possibility of the existence of another FABP-regulated factor from adipose tissue specifically targeting liver SCD-1 activity and development of fatty liver disease. Future studies should help to address these interesting prospects.

ACKNOWLEDGMENTS

G.S.H. has received National Institutes of Health Grant DK-64360 and grants from the Pew and American Diabetes Foundations. G.I.S. has received National Institutes of Health Grant U24-DK-59635. J.K.K. has received National Institutes of Health Grant U24-DK-59635 and American Diabetes Association Grant 7-01-JF-05. K.M. is recipient of a fellowship from Manpei Suzuki Diabetes Foundation. H.C. is recipient of a mentor-based fellowship from the American Diabetes Association.

Part of this study was conducted at the National Institutes of Health–Yale Mouse Metabolic Phenotyping Center.

REFERENCES

1. Haunerland NH, Spener F: Fatty acid-binding proteins: insights from genetic manipulations. *Prog Lipid Res* 43:328–349, 2004
2. Makowski L, Hotamisligil GS: Fatty acid binding proteins: the evolutionary crossroads of inflammatory and metabolic responses. *J Nutr* 134:2464S–2468S, 2004

3. Glatz JF, van der Vusse GJ: Cellular fatty acid-binding proteins: their function and physiological significance. *Prog Lipid Res* 35:243–282, 1996
4. Hanhoff T, Lucke C, Spener F: Insights into binding of fatty acids by fatty acid binding proteins. *Mol Cell Biochem* 239:45–54, 2002
5. Makowski L, Boord JB, Maeda K, Babaev VR, Uysal KT, Morgan MA, Parker RA, Suttles J, Fazio S, Hotamisligil GS, Linton MF: Lack of macrophage fatty-acid-binding protein aP2 protects mice deficient in apolipoprotein E against atherosclerosis. *Nat Med* 7:699–705, 2001
6. Zimmer JS, Dyckes DF, Bernlohr DA, Murphy RC: Fatty acid binding proteins stabilize leukotriene A4: competition with arachidonic acid but not other lipoxygenase products. *J Lipid Res* 45:2138–2144, 2004
7. Hotamisligil GS, Johnson RS, Distel RJ, Ellis R, Papaioannou VE, Spiegelman BM: Uncoupling of obesity from insulin resistance through a targeted mutation in aP2, the adipocyte fatty acid binding protein. *Science* 274:1377–1379, 1996
8. Uysal KT, Wiesbrock SM, Marino MW, Hotamisligil GS: Protection from obesity-induced insulin resistance in mice lacking TNF-alpha function. *Nature* 389:610–614, 1997
9. Boord JB, Maeda K, Makowski L, Babaev VR, Fazio S, Linton MF, Hotamisligil GS: Adipocyte fatty acid-binding protein, aP2, alters late atherosclerotic lesion formation in severe hypercholesterolemia. *Arterioscler Thromb Vasc Biol* 22:1686–1691, 2002
10. Maeda K, Uysal KT, Makowski L, Gorgun CZ, Atsumi G, Parker RA, Bruning J, Hertzel AV, Bernlohr DA, Hotamisligil GS: Role of the fatty acid binding protein mal1 in obesity and insulin resistance. *Diabetes* 52:300–307, 2003
11. Scheja L, Makowski L, Uysal KT, Wiesbrock SM, Shimshek DR, Meyers DS, Morgan M, Parker RA, Hotamisligil GS: Altered insulin secretion associated with reduced lipolytic efficiency in aP2$^{-/-}$ mice. *Diabetes* 48:1987–1994, 1999
12. Maeda K, Cao H, Kono K, Gorgun CZ, Furuhashi M, Uysal KT, Cao Q, Atsumi G, Malone H, Krishnan B, Minokoshi Y, Kahn BB, Parker RA, Hotamisligil GS: Adipocyte/macrophage fatty acid binding proteins control integrated metabolic responses in obesity and diabetes. *Cell Metab* 1:107–119, 2005
13. Boord JB, Maeda K, Makowski L, Babaev VR, Fazio S, Linton MF, Hotamisligil GS: Combined adipocyte-macrophage fatty acid-binding protein deficiency improves metabolism, atherosclerosis, and survival in apolipoprotein E-deficient mice. *Circulation* 110:1492–1498, 2004
14. Minokoshi Y, Kim YB, Peroni OD, Fryer LG, Muller C, Carling D, Kahn BB: Leptin stimulates fatty-acid oxidation by activating AMP-activated protein kinase. *Nature* 415:339–343, 2002
15. Cohen P, Miyazaki M, Socci ND, Hagge-Greenberg A, Liedtke W, Soukas AA, Sharma R, Hudgins LC, Ntambi JM, Friedman JM: Role for stearoyl-CoA desaturase-1 in leptin-mediated weight loss. *Science* 297:240–243, 2002
16. Pelleymounter MA, Cullen MJ, Baker MB, Hecht R, Winters D, Boone T, Collins F: Effects of the obese gene product on body weight regulation in ob/ob mice. *Science* 269:540–543, 1995
17. Campfield LA, Smith FJ, Guisez Y, Devos R, Burn P: Recombinant mouse OB protein: evidence for a peripheral signal linking adiposity and central neural networks. *Science* 269:546–549, 1995
18. Zhang Y, Proenca R, Maffei M, Barone M, Leopold L, Friedman JM: Positional cloning of the mouse obese gene and its human homologue. *Nature* 372:425–432, 1994
19. Johnson RS, Sheng M, Greenberg ME, Kolodner RD, Papaioannou VE, Spiegelman BM: Targeting of nonexpressed genes in embryonic stem cells via homologous recombination. *Science* 245:1234–1236, 1989
20. Uysal KT, Scheja L, Wiesbrock SM, Bonner-Weir S, Hotamisligil GS: Improved glucose and lipid metabolism in genetically obese mice lacking aP2. *Endocrinology* 141:3388–3396, 2000
21. Kim JK, Michael MD, Previs SF, Peroni OD, Mauvais-Jarvis F, Neschen S, Kahn BB, Kahn CR, Shulman GI: Redistribution of substrates to adipose tissue promotes obesity in mice with selective insulin resistance in muscle. *J Clin Invest* 105:1791–1797, 2000
22. Sheng Z, Otani H, Brown MS, Goldstein JL: Independent regulation of sterol regulatory element-binding proteins 1 and 2 in hamster liver. *Proc Natl Acad Sci U S A* 92:935–938, 1995
23. Miyazaki M, Kim YC, Ntambi JM: A lipogenic diet in mice with a disruption of the stearoyl-CoA desaturase 1 gene reveals a stringent requirement of endogenous monounsaturated fatty acids for triglyceride synthesis. *J Lipid Res* 42:1018–1024, 2001
24. Yamauchi T, Kamon J, Minokoshi Y, Ito Y, Waki H, Uchida S, Yamashita S, Noda M, Kita S, Ueki K, Eto K, Akanuma Y, Froguel P, Foufelle F, Ferre P, Carling D, Kimura S, Nagai R, Kahn BB, Kadowaki T: Adiponectin stimulates glucose utilization and fatty-acid oxidation by activating AMP-activated protein kinase. *Nat Med* 8:1288–1295, 2002
25. Fruebis J, Tsao TS, Javorschi S, Ebbets-Reed D, Erickson MR, Yen FT, Bihain BE, Lodish HF: Proteolytic cleavage product of 30-kDa adipocyte complement-related protein increases fatty acid oxidation in muscle and causes weight loss in mice. *Proc Natl Acad Sci U S A* 98:2005–2010, 2001
26. Shklyaev S, Aslanidi G, Tennant M, Prima V, Kohlbrenner E, Kroutov V, Campbell-Thompson M, Crawford J, Shek EW, Scarpace PJ, Zolotukhin S: Sustained peripheral expression of transgene adiponectin offsets the development of diet-induced obesity in rats. *Proc Natl Acad Sci U S A* 100:14217–14222, 2003
27. Randle PJ, Garland PB, Hales CN, Newsholme EA: The glucose fatty-acid cycle: its role in insulin sensitivity and the metabolic disturbances of diabetes mellitus. *Lancet* 1:785–789, 1963
28. Boden G, Shulman GI: Free fatty acids in obesity and type 2 diabetes: defining their role in the development of insulin resistance and beta-cell dysfunction. *Eur J Clin Invest* 32 (Suppl. 3):14–23, 2002